Structural Engineering and Mechanics, *Vol. 63, No. 2 (2017) 171-180*
DOI: https://doi.org/10.12989/sem.2017.63.2.171

Instability analysis of viscoelastic CNTs surrounded by a thermo-elastic foundation

Saeed Amir*[1], Mehdi Khani[1], Ali Reza Shajari[2] and Pedram Dashti[1]

[1]*Department of Solid Mechanics, Faculty of Mechanical Engineering, University of Kashan, Kashan, Iran*
[2]*Mechanical Properties Research Lab (MPRL), Faculty of Mechanical Engineering, K.N. Toosi University of Technology, No. 17, Pardis St., Mollasadra Ave., Vanak Square, Tehran, Iran*

(Received July 20, 2016, Revised October 11, 2016, Accepted January 26, 2017)

Abstract. Static and dynamic instability of a viscoelastic carbon nanotube (CNT) embedded on a thermo-elastic foundation are investigated, in this research. The CNT is modeled based on Euler-Bernoulli beam (EBB) and nonlocal small scale elasticity theory is utilized to analyze the structure. Governing equations of the system are derived using Hamilton's principle and differential quadrature (DQ) method is applied to solve the partial differential equations. The effects of variable axial load and diverse boundary conditions on static/vibration instability are studied. To verify the result of the DQ method, the Galerkin weighted residual approach is used for the instability analysis. It is observed appropriate agreement for results of two different solution methods and satisfactory accuracy with those obtained in prior studies. The results of this work could be useful for engineers and designers in order to produce and design nano/micro structures in thermo-elastic medium.

Keywords: static and vibration analysis; viscoelastic; armchair and zigzag CNT; variable axial load; thermo-elastic foundation

1. Introduction

Since CNTs have been discovered by Iijima (1991) many researchers have studied about syntheses processes, different properties and their applications. There are some articles dealing with static and/or dynamic behaviors of micro/nano structures that include diverse kind of CNTs. Nonlinear vibration of double-walled carbon nanotubes (DWCNTs) based on Euler-Bernoulli beam (EBB) theory considering nonlocal elasticity theory and nonlinear van der Waals interactions was investigated by Fang *et al*. (2013). They considered clamped-clamped boundary conditions and used Hamilton's principle to drive nonlinear equations of motion. After using harmonic balance and Davidon-Fletcher-Powell methods to solve their equilibrium equations they concluded that nonlinear van der Waals force has important effect on natural frequency of DWCNT in comparison with nonlinear geometric terms. Ranjbartoreh *et al*. (2008) investigated axial stability of single and double walled carbon nanotubes (SWCNT/DWCNT) surrounded by an elastic medium in different buckling modes. They considered the van der Waals interactions between layers of DWCNTs. They showed that the critical axial force of DWCNT was larger than for SWCNT. Pradhan and Mandal (2013) showed the effects of nonlocal parameter, length and thickness of CNT, temperature changes on buckling, bending and vibration stability of CNT. They obtained equations of motion based on Timoshenko beam (TB) theory and finite element method (FEM) is used to solve them. Aydogdu (2012) investigated the axial vibration of SWCNT surrounded by an elastic medium foundation based on Eringen nonlocal small scale theory. The effects of diverse parameters such as stiffness of elastic foundation, nonlocal coefficient and different boundary conditions on axial vibration instability were presented in this study. Wang and Wang (2013) demonstrated the dependency of natural frequency of CNT on stiffness and mass density of elastic media, small scale coefficient and rotary inertia. Hamilton's principle was used to derive equilibrium equations which are based on Timoshenko beam, nonlocal, stress and strain gradient theories. Lei *et al*. (2013) simulated CNT as a mechanical structure with viscoelastic properties based on the nonlocal Timoshenko beam theory. They studied the bending vibration of nanotubes with different boundary conditions. The natural frequencies and frequency response functions (FRF) are investigated by using transfer function methods. The dynamic stability of SWCNT and DWCNT under dynamic axial loading based on shell model and energy method was studied by Ghorbanpour Arani *et al*. (2011). They considered the effect of small length scale using Eringen's model. Their results demonstrated that the local and nonlocal critical dynamic loads in the case of axial buckling of the DWCNT were greater than the critical static loads. Chang and Lee (2012) investigated the vibration of CNTs using nonlocal viscoelasticity theory. The complex frequencies in closed-form expression were obtained in terms of the damping ratio. According to their analysis, the natural frequency significantly depends on damping coefficient, nonlocal parameter, thermal field and elastic medium. Boehle *et al*. (2015) presented a model of an

*Corresponding author
E-mail: samir@kashanu.ac.ir; saeid_amir27111@yahoo.com

ISSN: 1225-4568 (Print), 1598-6217 (Online)

embedded CNT based composite strain sensor where was composed of a bundle of fiberglass fibers coated with CNT through a thermal chemical vapor deposition process. They used a numerical model to predict the strain response of a composite with embedded fuzzy fiber. Also, they compared numerical results with experimental data. The longitudinal output of the sensor from the model were observed nearly matched with the experimental results. Thermo-mechanical nonlinear postbuckling of functionally graded plates resting on Pasternak foundation according to hyperbolic shear deformation theory was presented by Chikh *et al*. (2016). The elastic properties of the material were considered based on sigmoid power law and varying across the thickness of the plate. In their work, they investigated the effects of the material, geometrical characteristics, temperature, boundary conditions, foundation stiffness and imperfection on the mechanical and thermal buckling and post-buckling of the functionally graded plates. Besseghier *et al*. (2015) studied nonlinear vibration properties of a zigzag SWCNT embedded in a polymer matrix where elastic foundation was simulated by Winkler-type model. They used harmonic balance method to drive the relation between deflection amplitudes and resonant frequencies of the SWCNT. They demonstrated graphically that the chirality of zigzag CNT as well as surrounding elastic medium play more important roles in the nonlinear vibration of the SWCNT.

In this study, the CNT is assumed to have nonlocal viscoelastic properties according to the Kelvin-Voigt and Eringen models and simulated as an Euler-Bernoulli beam theory. The Hamilton's principle is implemented to obtain equations of motion. The effect of armchair and zigzag structures of CNT, on the static/dynamic instability are investigated. The CNT is embedded in a thermo-elastic foundation and the effect of temperature changes on the instability of CNT is expressed also. The elastic boundary conditions with two linear elastic and torsional springs at the ends of the structure are considered to investigate the effects of resistance of these two springs on buckling load and natural frequency. It is expected that by increasing the resistance of both springs, elastic boundary conditions will behave as clamped conditions. It can be stated that as the effect of torsional springs are neglected and linear elastic coefficient increases, elastic boundary conditions will approach to simply supported conditions. According to this study while boundary conditions resist axial movements, thermal compressive force will influence the stability of tube. A variable compressive (polynomial and harmonic) loads are applied on the structure and the effects of the compressive loads on static and dynamic instability region of the CNT are presented. Finally the presented results are compared with results of other authors for validation. Elastic boundary conditions and variable compressive loads are some of the innovative pints in this article. The results of DQ approach are compared with results of the Galerkin solution for indication of the results accuracy.

2. Governing equations

2.1 Nonlocal elasticity theory of viscoelastic model

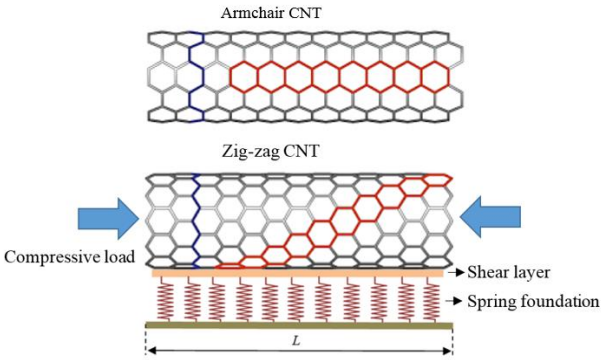

Fig. 1 A schematic figure of armchair and zigzag CNT stand on thermo-elastic foundation under an axial compressive load

Fig. 1 shows a CNT with length L surrounded by thermo-elastic medium subjected to an axial compressive load. Eringen expressed nonlocal continuum theory in which the stress tensor in a given point of the body is dependent to strain tensor in all points of the body. Due to discrete nature of nanostructures, using classical continuum mechanics for these structures have not been interested in recent studies. On the other hand, Nonlocal continuum theory, can be correlated with atomistic simulations of CNT and it gives acceptable results. Constitutive equations in nonlocal theory is expressed as (Reddy 2007)

$$\sigma(x) = E^* : \int_V \left(2\pi l'^2\right)^{-1} K_o\left(\frac{\sqrt{x.x}}{l'\tau}\right)\left(|x'-x|,\tau\right)T(x')dx', \quad (1)$$

where E^*, $T(x')$, l', K_0 and $|x'-x|$ are complex Young's modulus containing real and imaginary parts, local stress tenor, external characteristic size, modified Bessel function and Euclidean distance, respectively. Also $\tau=e_0a/l'$ in which e_0 and a are constants related to each material and interior features size, respectively.

The relation between nonlocal and classical stress tensors can be readily stated as (Ghorbanpour Arani *et al*. 2014)

$$\left[1-\tau^2 l'^2\nabla^2\right]\sigma^{nl} = T^l = E^* : \varepsilon. \quad (2)$$

Displacement field of the Euler-Bernoulli beam is given by (Ghorbanpour Arani *et al*. 2014)

$$\tilde{U}(x,z,t) = -z\frac{\partial W(x,t)}{\partial x}, \qquad \tilde{W}(x,z,t) = W(x,t). \quad (3)$$

where $\tilde{U}$ and $\tilde{W}$ are axial and transverse components of displacement vector of the beam throughout the thickness, U and W are axial and transverse displacements for midplane of the beam. According to the Green-Lagrange strain theory, the relations between strain tensor and displacement field are expressed as (Ghorbanpour Arani *et al*. 2014)

$$\varepsilon_{xx} = \frac{\partial \tilde{U}}{\partial x} = -z\,\frac{\partial^2 W}{\partial x^2},$$
$$\varepsilon_{xz} = \frac{1}{2}\left(\frac{\partial \tilde{W}}{\partial x} + \frac{\partial \tilde{U}}{\partial z}\right) = 0. \tag{4}$$

Implementing Kelvin-Voigt viscoelastic model, the rheological behavior of the system can be presented by two parameters: E and g, which indicate storage and loss factors, respectively. The nonlocal viscoelastic theory can be reduced as (Lei *et al*. 2013)

$$\sigma_{xx}^{nl} - (e_0 a)^2 \nabla^2 \sigma_{xx}^{nl} = E\left(1+g\frac{\partial}{\partial t}\right)\varepsilon_{xx} \xrightarrow{\int_A z dA}$$
$$M_{xx}^{nl} - (e_0 a)^2 \nabla^2 M_{xx}^{nl} = -EI\left(1+g\frac{\partial}{\partial t}\right)\frac{\partial^2 W}{\partial x^2}, \tag{5}$$

where M_{xx}^{nl} and denotes nonlocal in-plane bending moment of CNT

2.2 Energy method

To derive the governing equations, Energy principle and variational method is utilized. The governing equations of motion can be derived from the Hamilton's principle as following (Ghorbanpour Arani *et al*. 2014)

$$\int_{t_1}^{t_2} \delta\Pi dt = \int_{t_1}^{t_2} \left(\delta U_{starin} - \delta K_{total} - \delta W_{ext}\right) dt = 0. \tag{6}$$

Strain energy of the system with respect to the nonlocal small scale theory is expressed as (Ghannadpour *et al*. 2013)

$$U_s = \frac{1}{2}\int_V \sigma_{xx}^{nl}\varepsilon_{xx} dV = \frac{1}{2}\int_0^l \int_A \left(\sigma_{xx}^{nl}\varepsilon_{xx}\right) dA dx =$$
$$= \frac{1}{2}\int_0^L \int_A \left(-z\sigma_{xx}^{nl}\frac{\partial^2 W}{\partial x^2}\right) dA dx \xrightarrow{M_{xx}^{nl} = \int_A z\sigma_{xx}^{nl} dA}$$
$$U_s = \frac{1}{2}\int_0^L -M_{xx}^{nl}\frac{\partial^2 W}{\partial x^2} dx, \tag{7}$$

where L is length of nanotube. There are three kinds of external loads: axial thermal load created by uniform temperature changes, Pasternak foundation contributed transverse force and an axial compressive load. It was presented in Fig. 1 that elastic boundary conditions are applied at the ends of CNT which are considered in the external work term (Kiani 2013). The total external work on the system is given by

$$W_{ext} = \underbrace{\frac{1}{2}\int_0^L \left(2K_f W - 2G_f \frac{\partial^2 W}{\partial x^2}\right) W dx}_{\text{Pasternak foundation load}}$$
$$+ \underbrace{\frac{1}{2}\int_0^L \left(F_T\left(\frac{\partial W}{\partial x}\right)^2 + F_{pr}\left(\frac{\partial W}{\partial x}\right)^2\right) dx}_{CNT}$$
$$+ \underbrace{\frac{1}{2}\left(K_r\left(\frac{\partial W}{\partial x}\bigg|_{(L,t)}\right)^2 + K_W\left(W_{(L,t)}\right)^2\right)}_{\text{Elastic boundary condition}}, \tag{8}$$

where K_r, K_W, K_f and G_f are torsional stiffness, linear spring constant, temperature dependent foundation stiffness and shear coefficient of foundation, respectively. The parameters F_T=-$EA\alpha\Delta T$ (α is Thermal expansion constant) and F_{pr}=-P_b are compressive thermal load and compressive axial force, respectively. The CNT stands on an elastic temperature dependent foundation and its characteristics are presented in following equations (Shen and Zhang 2011)

$$\begin{cases} K_f = \dfrac{E_0\left(5-\left(2\gamma_1^2+6\gamma_1+5\right)\exp\left(-2\gamma_1\right)\right)}{4L\left(1-\upsilon_0^2\right)\left(2-c_1\right)^2} \\ c_1 = \left(\gamma_1+2\right)\exp\left(-\gamma_1\right) \\ \gamma_1 = \dfrac{H_s}{L};\ E_0 = \dfrac{E_f}{1-\upsilon_s^2};\ \upsilon_0 = \dfrac{\upsilon_f}{1-\upsilon_f}, \end{cases} . \tag{9}$$

where H_f=100 nm is the depth of foundation, υ_f=0.48 is the Poisson's ratio of foundation, E_s=3.22-0.0034T (Gpa) is temperature dependent Young's modulus of the foundation, T=T_0+ΔT is environment temperature and T_0=300K° is room temperature.

Total Kinetic energy of CNT can be obtained as follow (Ghannadpour *et al*. 2013, Ghorbanpour Arani *et al*. 2014)

$$K_{total} = \frac{1}{2}\rho_t \int_0^L \left(\int_{A_t}\left(\left(\frac{\partial \tilde{U}}{\partial t}\right)^2 + \left(\frac{\partial \tilde{W}}{\partial t}\right)^2\right) dA\right) dx$$
$$= \frac{1}{2}\rho_t \int_0^L \left(\int_{A_t}\left(\left(-z\,\frac{\partial^2 W}{\partial x\,\partial t}\right)^2 + \left(\frac{\partial W}{\partial t}\right)^2\right) dA\right) dx, \tag{10}$$

where ρ_t is density of CNT and $\left(m_t, I_t\right) = \int_{A_t} \rho_t\left(1, z^2\right) dA$, therefore Eq. (10) can be modified by these parameters

$$K_{total} = \frac{1}{2}\int_0^L \left(I_t\left(-\frac{\partial^2 W}{\partial x\,\partial t}\right)^2 + m_t\left(\frac{\partial W}{\partial t}\right)^2\right) dx. \tag{11}$$

2.3 Governing equation

Governing equations of the system can be obtained by using Hamilton's principle, substituting Eqs. (7)-(8) and (11) into Eq. (6), Equation of motion of CNT are obtained as

$$\int_{t_1}^{t_2}\delta\Pi\,dt=\int_{t_1}^{t_2}\left\{\int_0^L\left(-M_{xx}^{nl}\frac{\partial^2\delta W}{\partial x^2}+\left(2K_fW-2G_f\frac{\partial^2W}{\partial x^2}\right)\delta W+\left(F_t+F_{pr}\right)\frac{\partial W}{\partial x}\frac{\partial\delta W}{\partial x}-I_t\frac{\partial^2W}{\partial x\partial t}\frac{\partial^2\delta W}{\partial x\partial t}-m_t\frac{\partial W}{\partial t}\frac{\partial\delta W}{\partial t}\right)dx+K_r\frac{\partial W}{\partial x}\delta\left(\frac{\partial W}{\partial x}\right)+K_wW\delta(W)\right\}dt=0. \tag{12}$$

Eq. (12) is reduced to weak formulations as following

$$\int_{t_0}^{t}\left\{\int_0^L\left(-\frac{\partial^2M_{xx}^{nl}}{\partial x^2}+\left(2K_fW-2G_f\frac{\partial^2W}{\partial x^2}\right)-\frac{\partial}{\partial x}\left(\left(F_t+F_{pr}\right)\frac{\partial W}{\partial x}\right)+m_t\frac{\partial^2W}{\partial t^2}-I_t\frac{\partial^4W}{\partial x^2\partial t^2}\right)\delta W dx+\left(-M_{xx}^{nl}+K_r\frac{\partial W}{\partial x}-I_t\frac{\partial^2W}{\partial x\partial t}\right)\delta\left(\frac{\partial W}{\partial x}\right)\Big|_0^L+\left(K_wW+\frac{\partial M_{xx}^{nl}}{\partial u^2}\right)\delta(W)\Big|_0^L\right\}dt=0. \tag{13}$$

Using Eq. (13), the governing equations of the system with corresponding boundary conditions are obtained as

$$-\frac{\partial^2M_{xx}^{nl}}{\partial x^2}+\left(2K_fW-2G_f\frac{\partial^2W}{\partial x^2}\right)-\frac{\partial}{\partial x}\left(\left(F_t+F_{pr}\right)\frac{\partial W}{\partial x}\right)+m_t\frac{\partial^2W}{\partial t^2}-I_t\frac{\partial^4W}{\partial x^2\partial t^2}=0, \tag{14a}$$

And

$$\begin{cases}\left(-M_{xx}^{nl}+K_r\frac{\partial W}{\partial x}-I_t\frac{\partial^2W}{\partial x\partial t}\right)=0\ \text{or}\ \delta\left(\frac{\partial W}{\partial x}\right)=0,\\ \left(K_wW+\frac{\partial M_{xx}^{nl}}{\partial x}\right)=0\,\text{or}\,\delta(W)=0.\end{cases} \tag{14b}$$

According to Eq. (14-b), clamped boundary conditions will be reached as K_r and K_W approach to infinity. Here we substitute Eq. (5) into Eq. (14a) to estimate nonlocal moment of CNT (M_{xx}^{nl})

$$M_{xx}^{nl}=-EI\frac{\partial^2W}{\partial x^2}+\left(e_0a\right)^2\begin{pmatrix}2\left(K_fW-G_f\frac{\partial^2W}{\partial x^2}\right)-\\ \frac{\partial}{\partial x}\left(\left(F_t+F_{pr}\right)\frac{\partial W}{\partial x}\right)+m_t\frac{\partial^2W}{\partial t^2}-I_t\frac{\partial^4W}{\partial x^2\partial t^2}\end{pmatrix}. \tag{15}$$

Substituting Eq. (15) in Eq. (14a), the governing equation is obtained in terms of displacement component

$$EI\frac{\partial^4W}{\partial x^4}+EIg\frac{\partial^5W}{\partial x^4\partial t}+\left(2K_fW-2G_f\frac{\partial^2W}{\partial x^2}\right)-\frac{\partial}{\partial x}\left(\left(-EA\alpha\Delta T-P_b\right)\frac{\partial W}{\partial x}-EA\alpha\Delta Tg\frac{\partial^2W}{\partial x\partial t}\right)+m_t\frac{\partial^2W}{\partial t^2}-I_t\frac{\partial^4W}{\partial x^2\partial t^2}-\frac{\left(e_0a\right)^2\partial^2}{\partial x^2}\left(2\left(K_fW-G_f\frac{\partial^2W}{\partial x^2}\right)+m_t\frac{\partial^2W}{\partial t^2}-I_t\frac{\partial^4W}{\partial x^2\partial t^2}-\frac{\partial}{\partial x}\left(-EA\alpha\Delta T-P_b\right)\frac{\partial W}{\partial x}-EA\alpha\Delta Tg\frac{\partial^2W}{\partial x\partial t}\right)=0. \tag{16}$$

Eq. (16) can be presented in Non dimensional form, using dimensionless parameters, defined as follows

$$w=\frac{W}{R}\qquad \zeta=\frac{x}{L}\qquad \tau=\frac{t}{L^2}\sqrt{\frac{EI_t}{\rho_tA_t}}$$

$$en=\frac{e_0a}{L}\qquad \Delta\theta=\alpha\Delta T\qquad g_f=\frac{G_fL^2}{EI_t}$$

$$k_f=\frac{K_fL^4}{EI_t}\qquad A_t'=\frac{A_tL^2}{I_t}\qquad I_t'=\frac{I_t}{A_tL^2}$$

$$B_1=\frac{K_rL}{EI_t}\qquad B_2=\frac{K_wL^3}{EI_t}\qquad g^*=\frac{g}{L^2}\sqrt{\frac{EI_t}{\rho_tA_t}}$$

$$p_b=\frac{P_bL^2}{EI_t},$$

where R is radius of the CNT. Radius of the zigzag and armchair CNT can be obtained by $\left(R=0.142p\sqrt{3}/2\pi\right)$ nm and $\left(R=0.426p/2\pi\right)$ nm, respectively, where p is chiral index (Chang *et al*. 2005, Gafour *et al*. 2013).

Non dimensional governing equation is obtained by substituting dimensionless parameters in Eq. (16)

$$\frac{\partial^4w}{\partial\zeta^4}+g^*\frac{\partial^5w}{\partial\zeta^4\partial\tau}-\frac{\partial}{\partial\zeta}\left(\left(-A_t'\Delta\theta-p_b\right)\frac{\partial w}{\partial\zeta}-A_t'\alpha\Delta\theta g^*\frac{\partial^2w}{\partial\zeta\partial\tau}\right)+\frac{\partial^2w}{\partial\tau^2}-I_t'\frac{\partial^4w}{\partial\zeta^2\partial\tau^2}+2k_fw-2g_f\frac{\partial^2w}{\partial\zeta^2}-\frac{\left(en\right)^2\partial^2}{\partial\zeta^2}\left(-\frac{\partial}{\partial\zeta}\left(\left(-A_t'\Delta\theta-p_b\right)\frac{\partial w}{\partial\zeta}-A_t'\alpha\Delta\theta g^*\frac{\partial^2w}{\partial\zeta\partial\tau}\right)+\frac{\partial^2w}{\partial\tau^2}-I_t'\frac{\partial^4w}{\partial\zeta^2\partial\tau^2}+2k_fw-2g_f\frac{\partial^2w}{\partial\zeta^2}\right)=0. \tag{17}$$

3. Instability analysis

Eq. (17) is dimensionless equilibrium equation of viscoelastic CNT and the purpose of the present study is to

investigate static and dynamic instability regions of this structure. Galerkin and DQ are two prominent numerical methods used to solve Eq. (17). Appropriate accuracy and convergence are the most important benefits of these two numerical solution methods. They also require proportionally less computational time than other numerical methods such as finite element and finite difference methods.

Considering static instability of the structure, Eq. (17) can be reduced to

$$\frac{\partial^4 w}{\partial\zeta^4}-\frac{\partial}{\partial\zeta}\left(\left(-A_t'\Delta\theta-p_b\right)\frac{\partial w}{\partial\zeta}\right)+2k_f w-2g_f\frac{\partial^2 w}{\partial\zeta^2}$$
$$-\frac{(en)^2\partial^2}{\partial\zeta^2}\left(-\frac{\partial}{\partial\zeta}\left(\left(-A_t'\Delta\theta-p_b\right)\frac{\partial w}{\partial\zeta}\right)\right. \quad (18)$$
$$\left.+2k_f w-2g_f\frac{\partial^2 w}{\partial\zeta^2}\right)=0.$$

According to DQ method, the differential terms are approximated at some special points in the solution domain and the partial differential equations such as Eq. (18) or Eq. (17) can be converted to algebraic forms. In this method, the function w and its derivatives can be approximated as (Yang *et al*. 2010)

$$\left.\frac{\partial^m w}{\partial\zeta^m}\right|_{\zeta=\zeta_i}=\sum_{k=1}^{N}C_{ik}^{(m)}w_k,\quad i=1,2,...,N \quad (19)$$

Where N is the grid points along ζ and $C_{ik}^{(m)}$ is weighting coefficient matrix and its 'm'*th* derivative. The solution of the static equation (Eq. (18)) are obtained as follows (Ghorbanpour Arani *et al*. 2014, Yang *et al*. 2010)

$$\sum_{k=1}^{N}C_{ik}^4w_k-\left(-A_t'\Delta\theta-p_b\right)\sum_{k=1}^{N}C_{ik}^2w_k+2k_f\sum_{k=1}^{N}I_{ik}w_k$$
$$-2g_f\sum_{k=1}^{N}C_{ik}^2w_k-2(en)^2k_f\sum_{k=1}^{N}C_{ik}^2w_k \quad (20)$$
$$+2(en)^2g_f\sum_{k=1}^{N}C_{ik}^4w_k+(en)^2\left(-A_t'\Delta\theta-p_b\right)\sum_{k=1}^{N}C_{ik}^4w_k=0,$$
$$i=1,2,...,N$$

where 'I' is unit matrix. Boundary conditions can be converted to algebraic equations by using DQ method, also

$$\begin{cases}\left(\sum_{k=1}^{N}C_{ik}^2w_k+B_1\sum_{k=1}^{N}C_{ik}w_k\right)=0\ \text{or}\ \left(\sum_{k=1}^{N}C_{ik}w_k\right)=0\\ \left(B_2\sum_{k=1}^{N}I_{ik}w_k-\sum_{k=1}^{N}C_{ik}^3w_k\right)=0\ \text{or}\ \left(\sum_{k=1}^{N}I_{ik}w_k\right)=0\end{cases},\ i=1\text{or N} \quad (21)$$

Combining Eqs. (20) and (21), a set of algebraic equations can be obtained as

$$\left(\underbrace{\begin{bmatrix}K_{bb} & K_{bd}\\ K_{db} & K_{dd}\end{bmatrix}}_{[K]}+p_b\underbrace{\begin{bmatrix}K'_{bb}=[0] & K'_{bd}=[0]\\ K'_{db} & K'_{dd}\end{bmatrix}}_{[K']}\right)\begin{Bmatrix}w_b\\ w_d\end{Bmatrix}=0 \quad (22)$$

where [*K*] and [*K'*] are the stiffness matrix and stiffness matrix related to dimensionless critical buckling load (p_b), respectively. Dynamic instability solution can be investigated by solving dynamic equilibrium equation (Eq. (17)).The general solution of this equation can be obtained by separation of variables as following

$$w(\zeta,\tau)=w(\zeta)e^{\omega\tau} \quad (23)$$

where $\omega=\lambda\sqrt{EI_t/\rho_tA_t}/L^2$ is the dimensionless natural frequency in which λ is the natural frequency of CNT. Applying DQ method to the governing equations in dynamic form, a set of algebraic equations containing the natural frequency are achieved as

$$\left(\underbrace{\begin{bmatrix}M_{bb}=[0] & M_{bd}=[0]\\ M_{db} & M_{dd}\end{bmatrix}}_{[M]}\omega^2+\underbrace{\begin{bmatrix}D_{bb}=[0] & D_{bd}=[0]\\ D_{db} & D_{dd}\end{bmatrix}}_{[D]}\omega+\underbrace{\begin{bmatrix}K_{bb} & K_{bd}\\ K_{db} & K_{dd}\end{bmatrix}}_{[K]}\right)\begin{Bmatrix}w_b\\ w_d\end{Bmatrix}=0, \quad (24)$$

Where [*K*], [*D*] and [*M*] are the stiffness, damping and mass matrices, respectively. Natural frequency Eq. (24) can be calculated by space state theory (Ghorbanpour Arani *et al*. 2014, Yang *et al*. 2010). Imaginary part of eigenvalue (ω) is structural natural and real part of eigenvalue (ω) express structural damping frequencies of CNT.

4. Numerical results and discussion

In this section, influences of various parameters such as thermal effect, structural damping based on Kelvin-Voigt theory, small scale, elastic boundary conditions, thermo-elastic foundation and different axial loads, are investigated

Table 1 Variety of elasticity and shear modulus of CNTs in different temperature according to kinds of rolling procedure (Shen and Zhang 2011, Zhang and Shen 2006)

Rolling procedure	Type of CNT	Radius (nm)	Thickness	Temperature (K^o)	Young's modulus (Tpa)	Shear modulus (Tpa)
Armchair	(10,10)	0.678	0.067	300	5.65	1.94
				500	5.53	1.96
				700	5.47	1.96
Armchair	(12,12)	0.8136	0.067	300	5.53	1.9
				500	5.38	1.94
				700	5.34	1.95
Zigzag	(17,0)	0.6654	0.088	300	3.9	1.36
				500	3.89	1.36
				700	3.86	1.42
Zigzag	(21,0)	0.822	0.087	300	3.81	1.37
				500	3.79	1.4
				700	3.78	1.41

Table 2 Dimensionless critical buckling load and natural frequency of CNT with different boundary conditions and nonlocal constant

$\frac{e_0 a}{L}$	Ref.	Boundary Conditions		
		S-S	C-S	C-C
Vibration analysis, (Im(ω))				
0	(Kiani 2013)	9.8696	15.4182	22.3733
	(Wang *et al*. 2007)	9.8697	15.4182	22.3733
	(Pradhan and Phadikar 2009)	9.8696	15.4182	22.3733
	Present work	9.8696	15.4182	22.3733
0.5	(Kiani 2013)	5.3003	7.7837	10.9914
	(Wang *et al*. 2007)	5.3001	7.7835	10.9912
	Present work	5.30026	7.7837	10.9914
0.7	(Kiani 2013)	4.0854	5.9362	8.3483
	(Wang *et al*. 2007)	4.0852	5.9360	8.3481
	Present work	4.0854	5.9362	8.3483
Buckling analysis, P_b				
0	(Kiani 2013)	9.8696	20.1907	39.4784
	(Wang *et al*. 2006)	9.8695	20.1997	39.4786
	(Pradhan and Phadikar 2009)	9.8696	20.1907	39.4784
	Present work	9.8696	20.1907	39.4784
0.2	(Kiani 2013)	7.076	11.1697	15.3068
	(Wang *et al*. 2006)	7.076	11.1699	15.3068
	Present work	7.076	11.1697	15.3068
1	(Kiani 2013)	0.9080	0.9528	0.9753
	(Pradhan and Phadikar 2009)	0.9080	0.9528	0.9753
	Present work	0.9080	0.9528	0.9753

on static and dynamic instability of the structure. The characteristics of the CNT structure (Shen and Zhang 2011, Zhang and Shen 2006) are presented in Table 1 and the accuracy of the results is validated by Refs. (Ghannadpour *et al*. 2013, Pradhan and Phadikar 2009, Wang *et al*. 2007, Wang *et al*. 2006) in Table 2.

It is worth mentioning that by simplifying Eq. (17), equilibrium equations of Ref. (Ghannadpour *et al*. 2013) can be obtained also. Verification of the DQ numerical solution is expressed by comparing the results of DQ method with Ritz method and other works in Table 2.

4.1 Buckling load analysis

In Figs. 2 and 3 we discuss about the static instability region of structure and the effects of some parameters on critical buckling load are investigated. It is obvious that increasing the length of CNT leads to decreasing critical buckling load. Figs. 2 and 3 indicate the effect of nonlocal

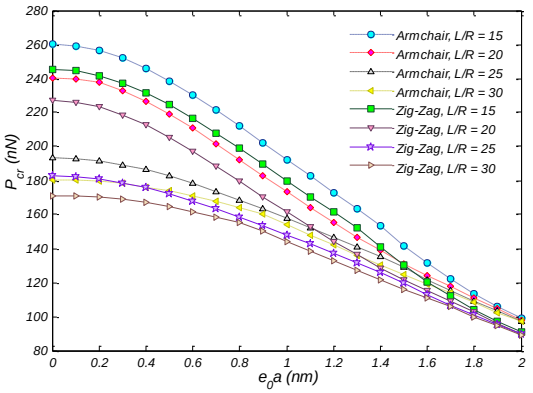

Fig. 2 Critical buckling load versus nonlocal parameter via different aspect ratios and clamped condition, $\Delta T = 0$

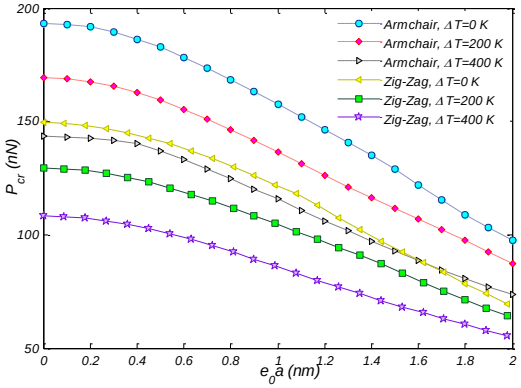

Fig. 3 Critical buckling load versus nonlocal parameter via diverse temperature and clamped conditions, *L/R*=25

small scale parameter on stability of the structure with various aspect ratios of CNT. As the nonlocal parameter increases, the stability region of CNT is decreased. As it is mentioned in Table1, temperature changes decrease Young's modulus of CNT and elastic coefficients of the foundation. The flexural rigidity of CNT decreases when Young's modulus is decreased. It is obvious that critical buckling load is in a direct relation with flexural rigidity of structures and stiffness of foundation, therefore temperature has a negative influence on static stability as can be seen in Fig. 3.

Figs. 4 and 5 are presented in order to have a comprehensive analysis on the effect of aspect ratio on the critical compressive load. Figs. 4 and 5 are based on various aspect ratios with different boundary conditions and diverse chirality, respectively. Clamped conditions always resist forces and moments while simply support conditions cannot resist moment load so every beams/tubes with clamped conditions at their boundaries are more stable than those with simply supported conditions. Fig. 4 illustrates this matter that structures with clamped-clamped conditions are the most stable beams/tubes and critical buckling load decreases while boundary conditions change from clamped-clamped to simply-simply supported conditions. Influence of chirality on the stability of CNT is demonstrated in Fig. 5

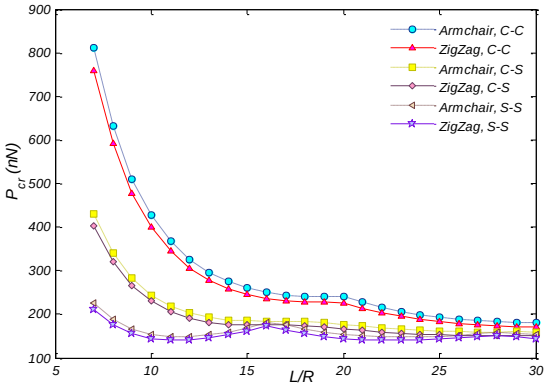

Fig. 4 Effects of various boundary conditions on critical buckling load versus aspect ratio, $\Delta T = 0$ and $e_0 a = 0$

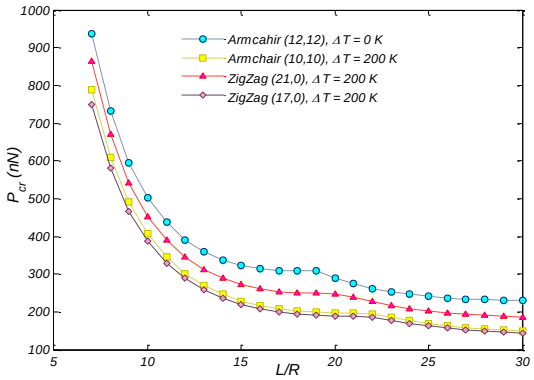

Fig. 5 Effects of different kind of rolling on buckling load versus aspect ratio with clamped conditions, $\Delta T = 0$ and $e_0 a = 0$

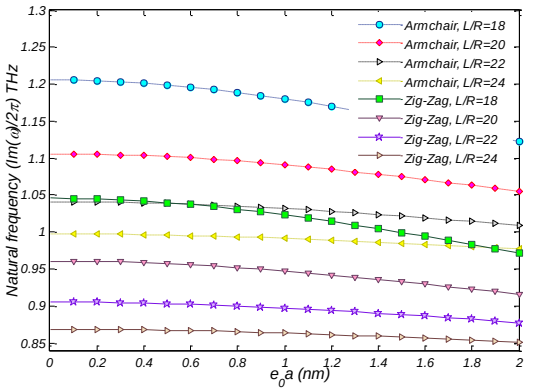

Fig. 6 Natural frequency versus nonlocal parameter via different aspect ratios and clamped condition, $\Delta T = 0$

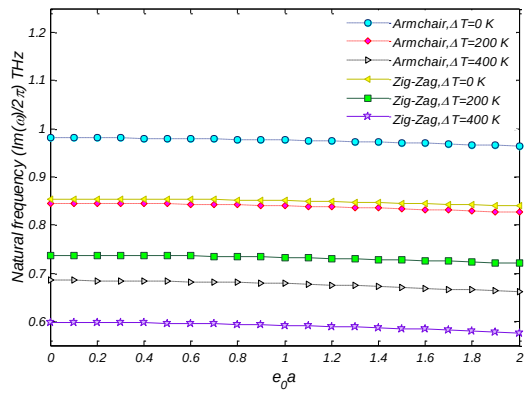

Fig. 7 Natural frequency versus nonlocal parameter via diverse temperature and clamped conditions, *L/R*=25

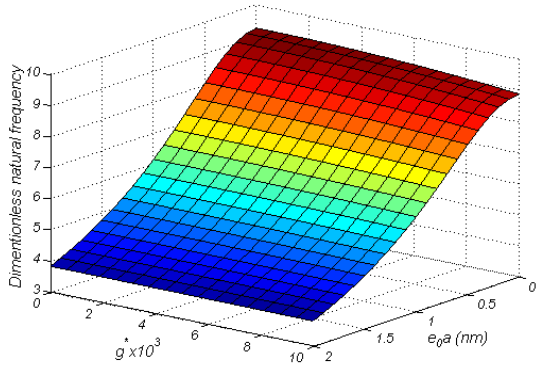

Fig. 8 Influence of nonlocal and viscoelastic parameter on dimensionless natural frequency for zigzag CNT with clamped conditions

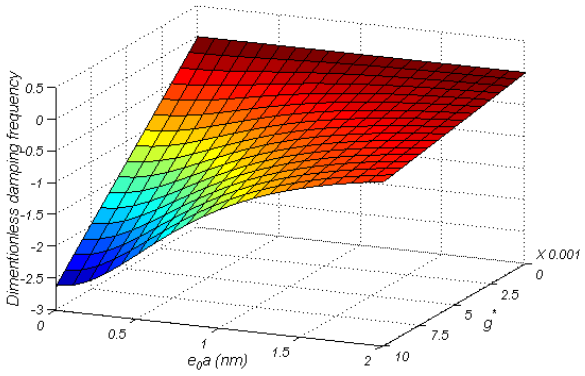

Fig. 9 Influence of nonlocal and viscoelastic parameter on dimensionless damping frequency for zigzag CNT with clamped conditions

and according to this figure, the Armchair structure is more stable statically than Zigzag.

4.2. Dynamical analysis

The effects of nonlocal parameter and temperature changes on natural frequency of the structure are illustrated in Figs. 6 and 7. Similar to buckling analysis, increasing nonlocal parameter and temperature changes, leads to decreasing the natural frequency and dynamic stability of the structure. Also natural frequency is dependent on flexural rigidity and corresponding parameters that decreases the flexural rigidity. Viscoelastic hypothesis is one of those theories that decreases flexural rigidity of

structures. The influence of Kelvin-Voigt viscoelastic parameters on natural frequency of CNTs with different chirality are illustrated in Figs. 8-11. These figures demonstrate the effects of viscoelastic parameter on dimensionless natural frequency and dimensionless damping frequency. These frequencies decrease because Kelvin-Voigt coefficient has a negative influence on flexural rigidity of structure.

The effects of elastic boundary conditions on natural frequency are illustrated in Figs. 12 and 13. Elastic boundary conditions is simulated by two springs, one resist transverse loads (B_2) and other resist moment loads (B_1).

It is expected that when both spring rigidity approach to infinity, elastic condition will be closed to clamped condition. Since no simply supported conditions can resist moment load so by increasing B_2 while B_1=0 elastic condition approaches to simply support condition. Results that are shown in Figs. 12 and 13 satisfy this matter.

Here, it is investigated the effects of two kinds of axial loads, that are function of 'x or ζ' (harmonic and polynomial dependent), on natural frequency of the presented model. According to Figs. 14 and 15 compressive loads decrease stability of structure while tension loads increase natural frequency of the CNT.

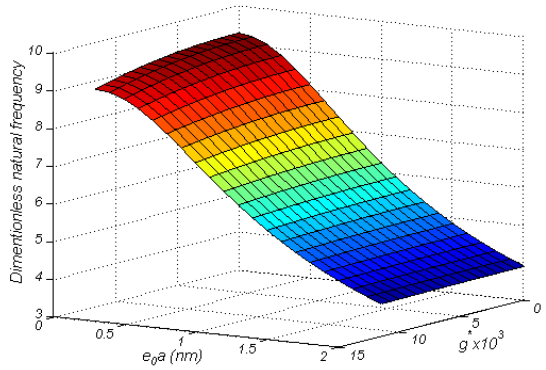

Fig. 10 Natural frequency versus nonlocal and viscoelastic parameter for armchair CNT with clamped conditions

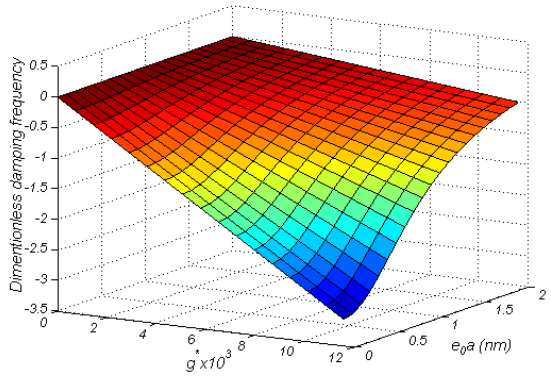

Fig. 11 Damping frequency versus nonlocal and viscoelastic parameter for armchair CNT with clamped conditions

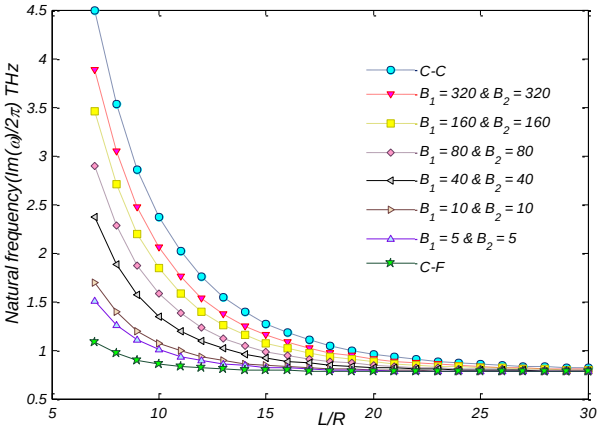

Fig. 12 Effects of suggested elastic boundary condition at the end of zigzag CNT on Natural frequency and $\Delta T = 0$

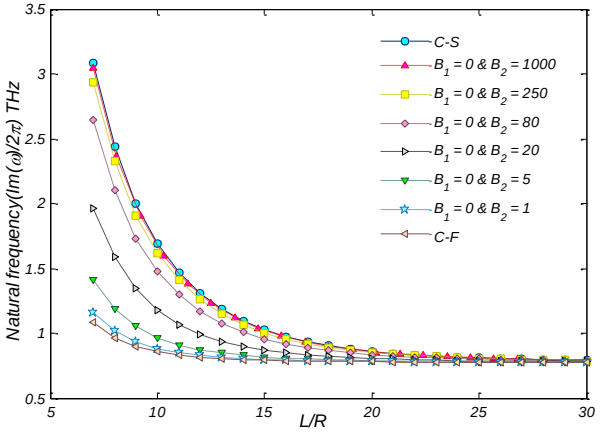

Fig. 13 Effects of suggested elastic boundary condition at the end of zigzag CNT on Natural frequency and $\Delta T = 0$

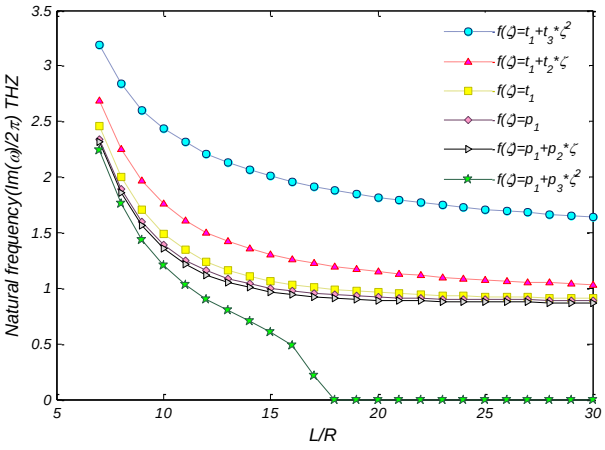

Fig. 14 Effects of polynomial axial load on Natural frequency of armchair CNT, t_1=20 nN, t_2=20 N/m, t_3=20 N/nm^2, p_1=-2 nN, $p_2 = -2\,N/m$, p_3=-2 N/nm^2 and ΔT=0

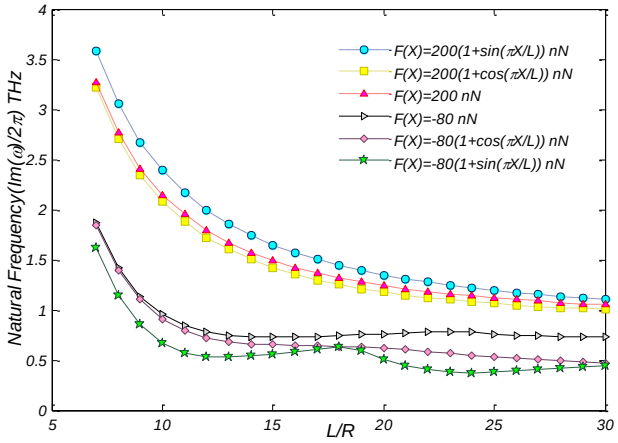

Fig. 15 Effects of harmonic axial load on Natural frequency of armchair CNT and $\Delta T = 0$

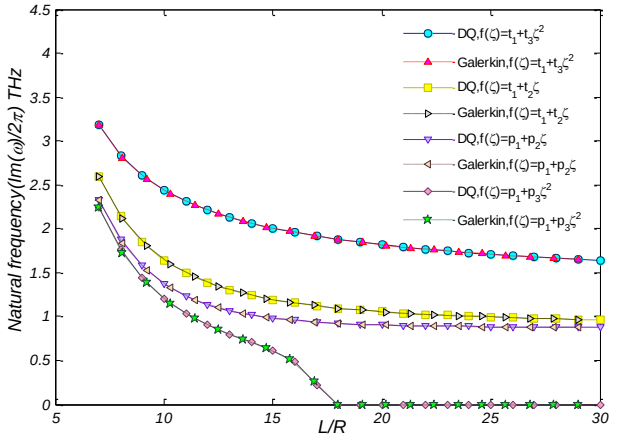

Fig. 16 Comparing the results of DQ method with Galerkin method for armchair CNT, t_1=20 nN, t_2=20 N/m, t_3=20 N/nm^2, p_1=-2 nN, $p_2 = -2\,N/m$, p_3=-2 N/nm^2 and ΔT=0

To verify the numerical solution, the Eq. (16) is solved with Galerkin method which examine a vibration deflection '$w(\zeta, \tau)$' as (Ghorbanpour Arani *et al*. 2014)

$$w\left(\zeta,\tau\right)=\sum_{i=1}^{N}Q_i\,\sin\left(i\,\pi\zeta\right)e^{\omega\tau}, \tag{25}$$

where Q_i and N are amplitude coefficient which are chosen sufficiently large integers. It is an essential matter that every suggested deflection must satisfy the boundary conditions. Substituting Eq. (25) into Eq. (16) and using Galerkin integral (Yoon *et al*. 2005), Eq. (16) will be converted to a set of algebraic equations as

$$\left(\left[M\right]\omega^2+\left[D\right]\omega+\left[K\right]\right)_{i\times i}\left\{Q_i\right\}_{i\times 1}=0. \tag{26}$$

Fig. 16 demonstrates accuracy of DQ method by comparing results of DQ with Galerkin method.

5. Conclusions

In this paper critical buckling load and natural frequency of viscoelastic CNT and influences of various parameters such as nonlocal coefficient, different boundary conditions, chirality of the CNT, Kelvin-Voigt viscoelastic constants and aspect ratio of the CNT were investigated. DQ method was used in order to solve static/dynamic governing equations and Galerkin method which is a prominent numerical solution was applied to validate the results of DQ method. Effects of elastic boundary conditions and variable axial loads on natural frequency and vibration instability of the CNT. The results had an appropriate accuracy and corresponded to results which were reported by prior articles. This article could be useful for engineers and designers in order to produce and design mechanical structures with more efficiency.

Acknowledgments

The authors would like to thank the reviewers for their valuable comments and suggestions to improve the clarity of this study. The authors are grateful to University of Kashan for supporting this work by Grant No. 539786/2. They would also like to thank the Iranian Nanotechnology Development Committee for their financial support.

References

Aydogdu, M. (2012), "Axial vibration analysis of nanorods (carbon nanotubes) embedded in an elastic medium using nonlocal elasticity", *Mech. Res. Commun*., **43**, 34-40.

Besseghier, A., Heireche, H., Bousahla, A.A., Tounsi, A. and Benzair, A. (2015), "Nonlinear vibration properties of a zigzag single-walled carbon nanotube embedded in a polymer matrix", *Adv. Nano Res*., **3**(1), 29-37.

Boehle, M., Pianca, P., Lafdi, K. and Chinesta, F. (2015), "Modeling of an embedded carbon nanotube based composite strain sensor", *Adv. Aircraft Spacecraft Sci*., **2**, 263–273.

Chang, T., Geng, J. and Guo, X. (2005), "Chirality- and size-dependent elastic properties of single-walled carbon nanotubes", *Appl. Phys. Lett*., **87**(25), 251929.

Chang, W. and Lee, H. (2012), "Vibration analysis of viscoelastic carbon nanotubes", *IET Micro Nano Lett*., **7**(12), 1308-1312.

Chikh, A., Bakora, A., Heireche, H., Houari, M.S.A., Tounsi, A. and Bedia, E.A. (2016), "Thermo-mechanical postbuckling of symmetric S-FGM plates resting on Pasternak elastic foundations using hyperbolic shear deformation theory", *Struct. Eng. Mech*., **57**(4), 617-639.

Fang, B., Zhen, Y.X., Zhang, C.P. and Tang, Y. (2013), "Nonlinear vibration analysis of double-walled carbon nanotubes based on nonlocal elasticity theory", *Appl. Math. Model*., **37**(3), 1096-1107.

Gafour, Y., Zidour, M., Tounsi, A., Heireche, H. and Semmah, A. (2013), "Sound wave propagation in zigzag double-walled carbon nanotubes embedded in an elastic medium using nonlocal elasticity theory", *Physica E*, **48**, 118-123.

Ghannadpour, S.A.M., Mohammadi, B. and Fazilati, J. (2013), "Bending, buckling and vibration problems of nonlocal Euler beams using Ritz method", *Compos. Struct*., **96**, 584-589.

Ghorbanpour Arani, A., Amir, S., Dashti, P. and Yousefi, M. (2014), "Flow-induced vibration of double bonded visco-CNTs

under magnetic fields considering surface effect", *Comput. Mater. Sci*., **86**, 144-154.
Ghorbanpour Arani, A., Hashemian, M., Loghman, A. and Mohammadimehr, M. (2011), "Study of dynamic stability of the double-walled carbon nanotube under axial loading embedded in an elastic medium by the energy method", *J. Appl. Mech. Tech. Phys*., **52**(5), 815-824.
Iijima, S. (1991), "Helical microtubules of graphitic carbon", *Nature*, **354**, 56-58.
Kiani, K. (2013), "Vibration analysis of elastically restrained double-walled carbon nanotubes on elastic foundation subjected to axial load using nonlocal shear deformable beam theories", *Int. J. Mech. Sci*., **68**, 16-34.
Lei, Y., Adhikari, S. and Friswell, M.I. (2013), "Vibration of nonlocal Kelvin-Voigt viscoelastic damped Timoshenko beam", *Int. J. Eng. Sci*., **66-67**, 1-13.
Pradhan, S.C. and Mandal, U. (2013), "Finite element analysis of CNTs based on nonlocal elasticity and Timoshenko beam theory including thermal effect", *Physica E*, **53**, 223-232.
Pradhan, S.C. and Phadikar, J.K. (2009), "Bending, buckling and vibration analyses of nonhomogeneous nanotubes using GDQ and nonlocal elasticity theory", *Struct. Eng. Mech.*, **33**(2), 193-213.
Ranjbartoreh, A.R., Wang, G.X., Ghorbanpour Arani, A. and Loghman, A. (2008), "Comparative consideration of axial stability of single- and double-walled carbon nanotube and its inner and outer tubes", *Physica E*, **41**(2), 202-208.
Reddy, J.N. (2007), "Nonlocal theories for bending , buckling and vibration of beams", *Int. J. Eng. Sci*., **45**(2), 288-307.
Shen, H.S. and Zhang, C.L. (2011), "Nonlocal beam model for nonlinear analysis of carbon nanotubes on elastomeric substrates", *Comput. Mater. Sci*., **50**(3), 1022-1029.
Wang, B.L. and Wang, K.F. (2013), "Vibration analysis of embedded nanotubes using nonlocal continuum theory", *Composites Part B*, **47**, 96-101.
Wang, C.M., Zhang, Y.Y. and He, X.Q. (2007), "Vibration of nonlocal Timoshenko beams", *Nanotechnology*, **18**(10), 105401.
Wang, C.M., Zhang, Y.Y., Ramesh, S.S. and Kitipornchai, S. (2006), "Buckling analysis of micro- and nano-rods/tubes based on nonlocal Timoshenko beam theory", *J. Phys. D: Appl. Phys*., **39**(17), 3904-3909.
Yang, J., Ke, L.L. and Kitipornchai, S. (2010), "Nonlinear free vibration of single-walled carbon nanotubes using nonlocal Timoshenko beam theory", *Physica E*, **42**(5), 1727-1735.
Yoon, J., Ru, C.Q. and Mioduchowski, A. (2005), "Vibration and instability of carbon nanotubes conveying fluid", *Compos. Sci. Technol*., **65**(9), 1326-1336.
Zhang, C.L. and Shen, H.S. (2006), "Temperature-dependent elastic properties of single-walled carbon nanotubes: Prediction from molecular dynamics simulation", *Appl. Phys. Lett*., **89**(8), 81904.